Rom J Morphol Embryol 2026, 67(2):243–248 ISSN (print) 1220–0522, ISSN (online) 2066–8279 doi: 10.47162/RJME.67.2.05

ORIGINAL PAPER

RJME Romanian Journal of Morphology & Embryology http://www.rjme.ro/

Mast cells – key players of digestive tumors associated angiogenesis

RALUCA ŞTEFANA IOANA MOŞ[1,2)], AMALIA-RALUCA CEAUŞU[1)], NELA-PUŞA GAJE[1)], VALERIA NICOLETA NĂSTASE[1)], ALEXANDRU CIOLOFAN[3)], ADELINA TUDOR[1)], IULIAN ALEXANDRU CIPRIAN BLIDIŞEL[3)], DIANA CARMEN MATCĂU[4)], ADINA OCTAVIA DUŞE[5)], AMALIA NICOLESCU[6)], MARIA DANIELA MOŢ[2)], ADINA LIGIA POP-MOLDOVAN[2)], LIANA MIOARA MOŞ[2)], OCTAVIAN MARIUS CREŢU[3)], FLAVIA ZARĂ[1)], OVIDIU ALEXANDRU MEDERLE[7)], MARIUS RAICA[1)]

[1)]*Department of Microscopic Morphology/Histology, Angiogenesis Research Center, Victor Babeş University of Medicine and Pharmacy, Timişoara, Romania*

[2)]*Department of Medicine, Vasile Goldiş Western University of Arad, Romania*

[3)]*Department of Surgical Semiology, Victor Babeş University of Medicine and Pharmacy, Timişoara, Romania*

[4)]*Department of Neurology, Victor Babeş University of Medicine and Pharmacy, Timişoara, Romania*

[5)]*Department of Balneology, Medical Rehabilitation and Rheumatology, Clinic of Physical Medicine, Balneology and Rheumatology, Transdisciplinary Research Center in Medical Rehabilitation, Balneology and Rheumatology, Victor Babeş University of Medicine and Pharmacy, Timişoara, Romania*

[6)]*Department of Intensive Care, Vasile Goldiş Western University of Arad, Romania*

[7)]*Department of Surgery, Victor Babeş University of Medicine and Pharmacy, Timişoara, Romania*

Abstract

Introduction: Mast cells (MCs) are immune cells derived from hematopoietic cluster of differentiation (CD)34+ and CD117+ precursors that complete their maturation in peripheral tissues such as the connective and mucosal layers, perivascular and perineural regions, and secondary lymphoid organs, where they play essential roles in regulating immune responses. The MC's dual role as both an effector and regulator of angiogenesis makes it a valuable indicator of tumor aggressiveness and a potential therapeutic target in digestive malignancies. *Materials and Methods*: 41 cases of digestive tumors with gastric, pancreatic and colorectal origins and their corresponding liver metastasis were evaluated by morphological and immunohistochemical techniques. The effects of Sodium Cromoglycate (Cromolyn) applied to a xenograft of cells derived from a liver metastasis of colorectal origin with a desmoplastic histological growth pattern, applied to chorioallantoic membrane (CAM) were analyzed. CD34 and mast cell tryptase (MCT) were used as primary antibodies. *Results*: A statistically significant correlation was noticed between mast cell density (MCD) outside the metastasis area and microvascular density (MVD) in the metastasis area with pancreatic origin (p=0.023). A statistically significant correlation was noted with a p-value of 0.046 for the desmoplastic histological growth pattern, between MCD in the metastatic area and the degree of differentiation. After therapy with Cromolyn, increased MVD and the absence of positive MCT were noticed in the xenograft. *Conclusions*: The analysis of MCD demonstrated marked variability depending on tumor type, differentiation, and histological growth pattern. Targeting MC activation could represent an adjuvant of anti-angiogenic therapy in metastatic digestive cancers.

Keywords: mast cells, microvascular density, digestive tumors, liver metastasis.

Introduction

Angiogenesis plays a pivotal role in the growth and metastatic potential of colorectal, gastric, and pancreatic tumors. In these malignancies, the activation of proangiogenic pathways, mainly mediated by vascular endothelial growth factor (VEGF), hypoxia-inducible factor 1-alpha (HIF-1α), and inflammatory cytokines, facilitate invasion and dissemination to distant organs. Once tumor cells colonize the liver, they adapt to the hepatic microenvironment through either neoangiogenesis or vessel co-option, generating distinct histological growth patterns. The resulting microvascular architecture of hepatic metastases reflects the interaction between tumor cells, endothelial cells, and stromal immune components such as mast cells (MCs), which can further modulate angiogenic activity [1, 2].

In gastric and colorectal cancers, increased MVD correlates with tumor progression, invasion, and metastasis. MCs and other stromal cells contribute to this process by releasing proangiogenic mediators such as tryptase and histamine. Among the various components of the tumor microenvironment, MCs play a pivotal role in cancer progression. MCs are now recognized as central elements of both innate and adaptive immunity. They rapidly release biologically active mediators, including histamine, proteases, and cytokines, that orchestrate inflammatory signaling and tissue remodeling through their ability to release a wide range of proangiogenic mediators such as VEGF, basic fibroblast growth factor (bFGF), tryptase, and chymase [3–5].

Through secretion of proangiogenic factors, MCs can enhance tumor vascularization and invasiveness. Conversely, they are also capable of releasing anti-tumor mediators,

This is an open-access article distributed under the terms of a Creative Commons Attribution-NonCommercial-ShareAlike 4.0 International Public License, which permits unrestricted use, adaptation, distribution and reproduction in any medium, non-commercially, provided the new creations are licensed under identical terms as the original work and the original work is properly cited.

suggesting a dual role in cancer progression [3, 6]. This dual functionality positions MCs as both potential promoters and regulators of tumor development, depending on the local microenvironmental context. In digestive malignancies, especially gastric and colorectal carcinomas and their hepatic metastases, elucidating this balance is critical to understanding how MCs contribute to the angiogenic switch and to identifying novel therapeutic targets within the tumor microenvironment [7, 8].

In digestive tract malignancies, particularly gastric and colorectal carcinomas, the density and activation status of MCs have been correlated with increased microvascular density (MVD), advanced tumor stage, and metastatic potential, especially toward the liver [5, 7, 9–11].

Aim

Based on these premises, we aimed to analyze the relationship between MCs and MVD and the histological growth patterns of liver metastases of colonic, gastric, and pancreatic origin.

Materials and Methods

The study included a total of 41 cases of digestive tumors with gastric, pancreatic and colorectal origins and their corresponding liver metastasis were evaluated by morphological and immunohistochemical (IHC) techniques. The samples were collected from patients treated at Municipal Emergency Clinical Hospital of Timişoara, Romania, between 2021–2025. The study was conducted with the patients' informed consent and the approval of the Ethics Committee of the Victor Babeş University of Medicine and Pharmacy, Timişoara (Approval No. 7339/22.04.2016). Data processing complied with the principles of the Declaration of Helsinki.

Primary processing

Tissue specimens obtained by open surgery were processed using standard histological techniques. Samples (<1 cm^3) were fixed in 10% neutral buffered formalin for 48 hours, washed in running water, dehydrated in graded ethanol, cleared in xylene, and embedded in paraffin using a ThermoScientific tissue processor. Sections of 3 μm thickness were cut, mounted on adhesive slides, and dried at 37°C.

Histochemical methods

For histopathological diagnosis, sections were stained with Hematoxylin–Eosin (HE). Morphological evaluation of HE-stained sections was followed by IHC investigations.

Immunohistochemistry

IHC staining was performed using the Leica Bond-Max automated immunostainer. The procedure included deparaffinization, antigen retrieval (Bond Epitope Retrieval Solutions 1 and 2, pH 6 and 9), peroxidase blocking, and incubation with the primary antibodies anti-cluster of differentiation 34 (CD34) (QBEnd10), anti-keratin 20 (K20) (clone Ks20.8) and anti-mast cell tryptase (MCT) (clone 10D11) all prediluted (Leica Biosystems). Visualization used the Bond Polymer Refine Detection System.

Quantification

MVD was assessed in three vascular "hot spots" at ×400 magnification according to Weidner's [12] method, and the mean value was recorded. Cytoplasmic expression was evaluated. Microscopic analysis and digital imaging were performed using a Grundium Ocus™ 40 digital microscope, and statistical analysis was carried out with Statistical Package for the Social Sciences (SPSS) 17.0, considering $p<0.05$ as significant.

Experimental model

Eggs were divided into two groups, each group containing 10 eggs, plus the control group and incubated at a temperature of 37°C, in a humid atmosphere. On the third day of incubation, a window was made on the surface of the egg and covered with adhesive tape. A silicone ring was applied to the surface of the chorioallantoic membrane (CAM) and a suspension of tumor cells derived from colorectal cancer liver metastasis (CRLM) (dHGP) was implanted.

Results

Hepatic metastasized primary colorectal tumors, which developed a desmoplastic growth pattern, were distributed as follows: well-differentiated (five cases), moderately differentiated (four cases), and poorly differentiated (three cases). Vascular morphology indicated the presence of vessels with wide, irregular lumens and vessels without lumens, with pillars, within the tumor areas. These features were observed in the tumor area. The average MVD in well-differentiated primary tumors analyzed showed values of 13.25 vessels. Peritumorally, vessels without lumens predominated, with an average density of 19.38. MVD in the metastatic area, for cases with a well-differentiated origin and desmoplastic growth pattern, was higher in the desmoplastic stroma compared with the metastatic area. Numerous vessels were observed in the desmoplastic stroma (average value of 17.52), with wide lumens, whereas intratumorally, vessels without lumens predominated, showing a lower MVD. The average values of MVD in the metastatic area for the desmoplastic growth model showed values of 11.79 vessels.

In the case of moderately differentiated colorectal tumors, the MVD had values of 15.35, while in the corresponding metastatic area, with a desmoplastic growth pattern, it showed values of 16.08 vessels. In the tumor area, vessels without a lumen or with a narrow, irregular lumen, with intraluminal pillars, were observed (Figure 1A). The corresponding metastasis presented vessels with a wide lumen, numerous in the desmoplastic zone and fewer (value of 25.58), predominantly without a lumen, inside the metastatic area (value of 16.08) (Figure 1B). Poorly differentiated tumors were characterized by a MVD value of 33, while the metastasis with a desmoplastic growth pattern had a value of 20.44. In the desmoplastic stroma, numerous vessels without lumens, showing intussusception phenomena, were noted.

In the metastatic area, vessels without lumen were observed, small in size, few in number, or with irregular, narrow lumen. In the portal spaces, numerous vessels without lumen and the presence of inflammatory infiltrate were identified. Summarizing, the average values of MVD for the primary tumors and the corresponding liver metastases, with a desmoplastic growth pattern, were highlighted in Table 1.

Table 1 – *Distribution of mean values of MVD*

Grade	ITUMVD	PERITUMVD	Grade	ITUMVD	PERITUMVD	Grade	ITUMVD	PERITUMVD
WDPRT	13.25	19.38	*MDPRT*	15.35	32.16	*PDPRT*	33	45
META desmoplastic type	11.79	17.52	*META desmoplastic type*	16.08	25.58	*META desmoplastic type*	20.44	31.50

Distribution of mean values of microvascular density (MVD) in well, moderately, and poorly differentiated colorectal adenocarcinomas and corresponding liver metastases (META) with a desmoplastic growth pattern. ITUMVD: Mean value of intratumoral MVD; MDPRT: Moderately differentiated primary tumor; PDPRT: Poorly differentiated primary tumor; PERITUMVD: Mean value of peritumoral MVD; WDPRT: Well-differentiated primary tumor.

Primary colorectal tumors that developed metastases with a pushing growth pattern had the following distribution: well-differentiated (three cases), moderately differentiated (five cases), poorly differentiated (four cases). Poorly differentiated primary tumors presented vessels with wide lumens, organized in networks, as well as numerous vessels without lumens (Figure 2A). The corresponding metastases were characterized by low MVD, small size, with narrow or absent lumens (Figure 2B). Moreover, dilation of the portal space vessels was observed. The average MVD in the metastatic area was 10.55 for well-differentiated tumors and 6.52 in the primary tumor. The corresponding values for metastases with a pushing growth pattern originating from moderately and poorly differentiated adenocarcinomas are shown in Table 2.

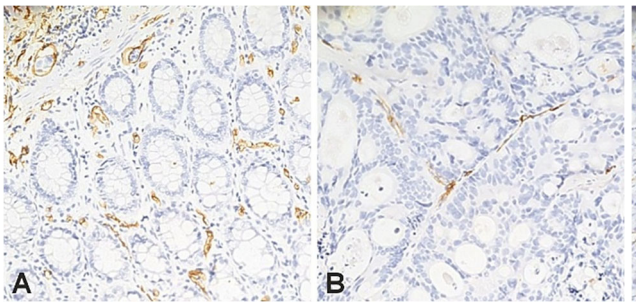

Figure 1 – *Moderately differentiated colon adenocarcinoma, morphology of the vessels in the primary tumor (A) and the corresponding metastasis (B). Anti-CD34 antibody immunostaining: (A) ×100; (B) ×200. CD34: Cluster of differentiation 34.*

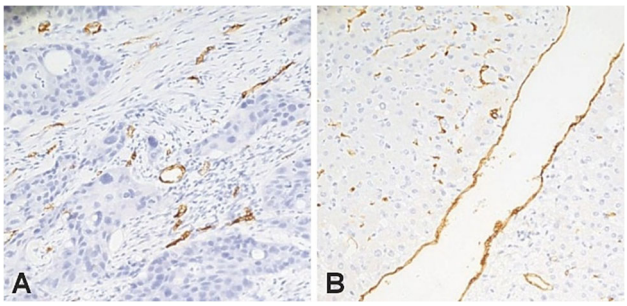

Figure 2 – *Poorly differentiated colorectal adenocarcinoma, intratumoral vascular morphology (A), corresponding metastasis – pushing growth pattern (B). Anti-CD34 antibody immunostaining: (A and B) ×200.*

Table 2 – *Distribution of mean MVD values*

Grade	ITUMVD	Grade	ITUMVD	Grade	ITUMVD
WDPRT	6.52	*MDPRT*	28.86	*PDPRT*	43.58
META pushing type	10.55	*META pushing type*	25.796	*META pushing type*	38.91

Distribution of mean microvascular density (MVD) values in well, moderately, and poorly differentiated colorectal adenocarcinomas and corresponding liver metastases (META) with a pushing growth pattern. ITUMVD: Mean value of intratumoral MVD; MDPRT: Moderately differentiated primary tumor; PDPRT: Poorly differentiated primary tumor; WDPRT: Well-differentiated primary tumor.

In the case of primary tumors that metastasized through a replacement growth pattern, the distribution was well-differentiated (three cases), moderately differentiated (one case), and poorly differentiated (two cases). The moderately and poorly differentiated cases showed a network arrangement of vessels with or without a lumen, periglandulary. The corresponding metastases, developed through a replacement growth pattern, maintained the vascular organization and distribution, but were more disorganized compared to the primary tumor. The values of the primary tumors and their corresponding metastases are presented in Table 3.

Table 3 – *The values of the primary tumors and their corresponding metastases (META)*

Grade	ITUMVD	Grade	ITUMVD	Grade	ITUMVD
WDPRT	7.74	*MDPRT*	40.30	*PDPRT*	23.66
META replacement type	9.88	*META replacement type*	62	*META replacement type*	44.66

The average microvascular density (MVD) value was 58.66. ITUMVD: Mean value of intratumoral MVD; MDPRT: Moderately differentiated primary tumor; PDPRT: Poorly differentiated primary tumor; WDPRT: Well-differentiated primary tumor.

The replacement growth model was the only type of model observed in liver metastases of pancreatic origin in our study (eight cases). In the portal spaces, inflammatory infiltrate and tumor cells were present. Areas with a "cord-like" appearance connecting the portal spaces and metastatic zones were also noticed.

Hepatic metastases included in our study (three cases), with gastric origin showed a pushing histological growth pattern. Inflammatory infiltrate and tumor cells were present in the portal spaces, and around these spaces, the presence of vessels with narrow lumens was noted. A particular aspect observed was CD34 expression in some of the hepatic sinusoids. The MVD value in the metastatic area was 105.33 in these cases.

Hepatic metastases originating from the colon and exhibiting a desmoplastic growth pattern were characterized by the presence of a large number of MCs in the portal spaces. Large sizes of these were observed and a predominance of

degranulated ones in poorly differentiated stages. Within the metastasis area, we noted a reduced number of MCs compared to the peritumoral region, with an average of 2.73 and 16, respectively.

One of the G1 cases was characterized by the absence of MCs in the metastatic area – desmoplastic type, while the other showed an average value of 1.33. The moderately differentiated cases were characterized by an average value of 2. The G3 cases had the highest number of MCs in the metastatic area, with an average value of 9.33. At the level of the remnant liver metastatic area, the presence of MCs majority was noted.

The growth-through-replacement model of hepatic metastases of colonic origin was characterized by a high density of MCs in areas around the metastatic site, with a density value of 20, compared to the metastatic area with an average value of 3.33.

In the pushing type growth model, the lowest number of MCs was noticed both at the boundary of the remaining liver metastasis (value of 5) and within the metastatic area itself (value of 1.99).

Cases of liver metastases of pancreatic origin were characterized by an average value of 2.85 mast cell density (MCD) within the metastatic area. In the surrounding zone of the metastatic area, the average MCD was 10.8.

Liver metastases of gastric origin (three cases), showing a pushing-type growth pattern and a moderate degree of differentiation, were characterized by a MCD value of 2.66 in the metastatic area. In the vicinity of the metastatic area, a MCD value of 3.66 was noted.

A statistically significant correlation was observed between MCD outside the metastasis area and MVD in the metastasis area with pancreatic origin (p=0.023).

A statistically significant correlation was noted with a p-value of 0.046 for the desmoplastic growth model, between MCD in the metastatic area and the degree of differentiation.

The analysis of MVD and MCD and the therapeutic impact was evaluated in an experimental model. A suspension of tumor cells derived from liver metastases of colonic origin was implanted on the CAM, in a ring. The metastasis began to acquire vessels from the neighboring CAM (Figure 3). After two days, when the tumor graft became visible, the first group was treated with 2 µL of Sodium Cromoglycate.

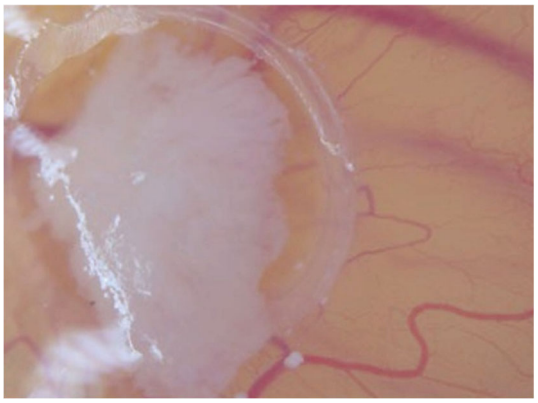

Figure 3 – ***Tumor cell suspension, in silicon ring, at the chorioallantoic membrane (CAM) level (×400).***

Morphological staining indicated a desmoplastic growth pattern of the liver metastasis originating from the colon. The colon localization of primary tumor was sustained by K20 positivity.

Analysis of CD34 expression indicated the presence of numerous tumor vessels of variable sizes, thin walled, mostly without lumen at the level of the metastatic area. Following therapy, increased MVD was noticed in the xenograft. Small vessels with thin walls and lumen were noticed, as well as small, non-permeable vessels (Figure 4, A and B).

At the level of metastasis, MCs were noticed in the immediate vicinity of the metastatic area. The presence of MCs was not noted in the xenograft treated with Sodium Cromoglycate (Figure 5, A and B).

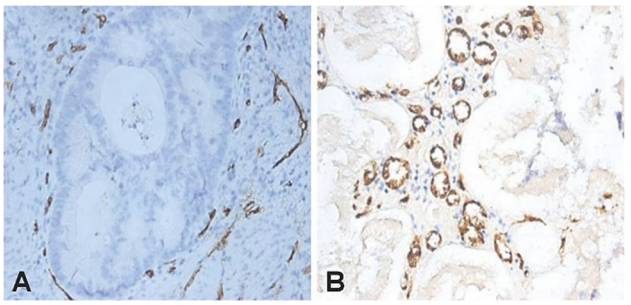

Figure 4 – ***CD34 immunostaining (×400) at the level of the metastasis (A) and the xenograft (B).***

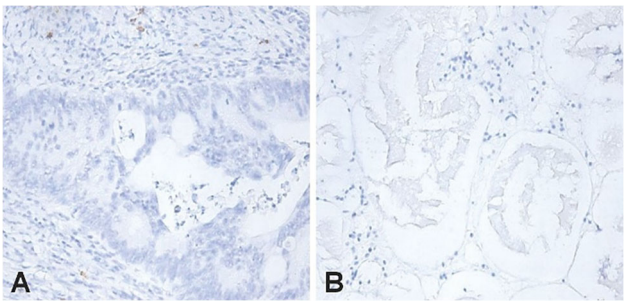

Figure 5 – ***Mast cell tryptase immunostaining (×400) at the level of the metastasis (A) and the xenograft (B).***

Discussions

The present study analyzed MVD and MC distribution in primary colorectal, gastric, and pancreatic tumors and their corresponding hepatic metastases, emphasizing the relationship between tumor differentiation, metastatic growth patterns, and stromal immune components.

Our findings indicate that MVD varies according to both tumor differentiation and metastatic growth pattern. In colorectal adenocarcinomas with a pushing growth pattern, primary tumors showed a more developed vascular network, characterized by wide-lumen vessels and numerous capillary-like structures. In contrast, their hepatic metastases exhibited reduced vascularization, with small-caliber or non-lumenized vessels, suggesting that once metastatic dissemination is established, the tumor may rely less on neoangiogenesis and more on vessel co-option from the host liver parenchyma. This observation is consistent with previous reports describing a shift from sprouting angiogenesis to vessel co-option in colorectal liver metastases [13].

Van den Eynden *et al.* [14] demonstrated that liver metastases of colorectal carcinomas with a replacement growth pattern are non-angiogenic, compared to liver metastases with a pushing-type growth pattern, which are highly angiogenic through a hypoxic mechanism. In metastases displaying a replacement growth pattern, the vascular architecture was largely preserved compared with the primary tumor, though more disorganized. This pattern reflects tumor cell infiltration along pre-existing hepatic sinusoids, a process that allows tumor expansion without the need for intense neoangiogenesis. Such replacement-type metastases are thought to be less responsive to anti-angiogenic therapy, since they exploit existing hepatic vessels instead of forming new ones.

Pancreatic metastases in our study exhibited exclusively a replacement pattern, with moderate MVD values and inflammatory infiltrate in portal spaces, consistent with their highly desmoplastic stroma and limited angiogenic potential. Gastric-origin metastases, conversely, displayed a pushing growth pattern and the highest MVD values among the analyzed groups. CD34 expression in hepatic sinusoids suggests reactive endothelial activation induced by tumor-secreted proangiogenic mediators, possibly VEGF and tryptase released by MCs.

The analysis of MCD demonstrated marked variability depending on tumor type, differentiation, and growth pattern. Desmoplastic metastases had abundant MCs in the peritumoral stroma, especially in poorly differentiated cases, confirming the involvement of MCs in the modulation of fibrosis and angiogenesis through the release of proteases and cytokines. The positive correlation between MCD and MVD, particularly in pancreatic metastases (p=0.023), supports the concept of a MC-driven angiogenic micro-environment, where MC degranulation promotes endothelial activation and vessel remodeling.

The correlations obtained by Ammendola *et al.* [15] between angiogenesis, MCD in bone metastases originating from gastric cancer, support the idea that at the bone tissue level, the development of metastases is favored by MCT+ MCs, which enhance angiogenesis.

In pushing-type metastases, both intra- and perimetastatic MC numbers were low, possibly reflecting a less inflamed, more compact stromal interface, while replacement-type metastases showed higher MC densities around the metastatic borders, where tumor cells interact with host sinusoids. These findings reinforce the idea that MCs may facilitate vascular adaptation at the invasive margin, depending on the mode of metastatic invasion.

The observed correlation between MCD and the degree of differentiation (p=0.046) further suggests that MC infiltration increases with tumor dedifferentiation and aggressiveness. This aligns with studies reporting higher MC counts in poorly differentiated gastrointestinal carcinomas and their metastases, where MCs contribute to angiogenic switching and extracellular matrix remodeling.

The experimental CAM model confirmed that tumor cells derived from hepatic metastases of colonic origin can rapidly acquire vessels from the host tissue, and that MC stabilization with Sodium Cromoglycate may reduce angiogenic activity. This supports the hypothesis that targeting MC activation could represent an adjunctive anti-angiogenic strategy in metastatic digestive cancers.

Overall, our data demonstrates a complex interplay between MVD, MC infiltration, and metastatic growth pattern, emphasizing that the angiogenic profile of hepatic metastases is not uniform but depends on both tumor origin and stromal interaction. The identification of these patterns may have therapeutic implications, particularly for the selection of patients likely to respond to anti-angiogenic or MC-targeted therapy.

The identification of angiogenic and inflammatory mechanisms in digestive tumors provides new opportunities for targeted therapy beyond conventional cytotoxic regimens. Our findings emphasize the contribution of MCs and endothelial activation in shaping the vascular micro-environment of colorectal, gastric, and pancreatic carcinomas, as well as their hepatic metastases. These observations support the logic behind combining MC stabilizers such as Sodium Cromoglycate with anti-angiogenic or tyrosine kinase-targeted agents to modulate tumor progression.

Sodium Cromoglycate acts by inhibiting MC degranulation, thereby reducing the release of histamine, tryptase, and VEGF, key mediators of angiogenesis and vascular permeability. Experimental models, including the CAM assay used in this study, demonstrated a visible reduction in neovascularization following Cromoglycate administration, confirming its potential anti-angiogenic effect. Although not currently integrated into oncological protocols, the drug's excellent safety profile makes it an attractive candidate for adjunctive therapy aimed at limiting MC-driven angiogenesis and tumor–stroma interactions [16].

Data from the literature have demonstrated a reduction in the growth, expansion, and survival of pancreatic and endothelial cells in an *in vivo* experimental model, at the level of the CAM of the embryonic egg, in the case of application of a MC degranulation inhibitor, Cromolyn [17, 18].

Conclusions

The use of MCs inhibitors in the therapy of hepatic metastases with a desmoplastic growth pattern may be an effective therapeutic solution. Taken together, the combined modulation of MC-mediated inflammation and tyrosine kinase signaling could represent a promising integrative approach in digestive cancers with liver metastasis.

Conflict of interests

The authors declare that they have no conflict of interests.

References

[1] Liu X, Li X, Wei H, Liu Y, Li N. Mast cells in colorectal cancer tumour progression, angiogenesis, and lymphangiogenesis. Front Immunol, 2023, 14:1209056. https://doi.org/10.3389/fimmu.2023.1209056 PMID: 37497234 PMCID: PMC10366593

[2] Fleischer JR, Schmitt AM, Haas G, Xu X, Zeisberg EM, Bohnenberger H, Küffer S, Teuwen LA, Karras PJ, Beißbarth T, Bleckmann A, Planque M, Fendt SM, Vermeulen P, Ghadimi M, Kalucka J, De Oliveira T, Conradi LC. Molecular differences of angiogenic *versus* vessel co-opting colorectal cancer liver metastases at single-cell resolution. Mol Cancer, 2023, 22(1):17. https://doi.org/10.1186/s12943-023-01713-1 PMID: 36691028 PMCID: PMC9872436

[3] Ligan C, Ma XH, Zhao SL, Zhao W. The regulatory role and mechanism of mast cells in tumor microenvironment. Am J Cancer Res, 2024, 14(1):1–15. https://doi.org/10.62347/ezst5505 PMID: 38323271 PMCID: PMC10839313

[4] Guo J, Chen J, Wang Y, Bai X, Feng H, Sheng S, Wang H, Xu K, Huang M, Lei Z, Chu X. Putative function and prognostic molecular marker of mast cells in colorectal cancer. BMC Med Genomics, 2025, 18(1):65. https://doi.org/10.1186/s12920-025-02117-4 PMID: 40205370 PMCID: PMC11983841
[5] Ali E, Červenková L, Pálek R, Ambrozkiewicz F, Hošek P, Daum O, Liška V, Hemminki K, Trailin A. Prognostic role of macrophages and mast cells in the microenvironment of hepatocellular carcinoma after resection. BMC Cancer, 2024, 24(1):142. https://doi.org/10.1186/s12885-024-11904-8 PMID: 38287290 PMCID: PMC10823625
[6] Albano F, Severini FL, Calice G, Zoppoli P, Falco G, Notarangelo T. The role of the tumor microenvironment and inflammatory pathways in driving drug resistance in gastric cancer: a systematic review and meta-analysis. Biochim Biophys Acta Mol Basis Dis, 2025, 1871(10):167821. https://doi.org/10.1016/j.bbadis.2025.167821 PMID: 40203956
[7] Shu F, Yu J, Liu Y, Wang F, Gou G, Wen M, Luo C, Lu X, Hu Y, Du Q, Xu J, Xie R. Mast cells: key players in digestive system tumors and their interactions with immune cells. Cell Death Discov, 2025, 11(1):8. https://doi.org/10.1038/s41420-024-02258-y PMID: 39814702 PMCID: PMC11735678
[8] Segura-Villalobos D, Ramírez-Moreno IG, Martínez-Aguilar M, Ibarra-Sánchez A, Muñoz-Bello JO, Anaya-Rubio I, Padilla A, Macías-Silva M, Lizano M, González-Espinosa C. Mast cell–tumor interactions: molecular mechanisms of recruitment, intratumoral communication and potential therapeutic targets for tumor growth. Cells, 2022, 11(3):349. https://doi.org/10.3390/cells11030349 PMID: 35159157 PMCID: PMC8834237
[9] Nishi M, Yamashita S, Takasu C, Wada Y, Yoshikawa K, Tokunaga T, Nakao T, Kashihara H, Yoshimoto T, Shimada M. Role of mast cell in locally advanced rectal cancer treated with neoadjuvant chemoradiotherapy. BMC Cancer, 2025, 25(1):99. https://doi.org/10.1186/s12885-025-13458-9 PMID: 39825280 PMCID: PMC11740561
[10] Qiao T, Ding C, Yu S, Li W, Zhao Y, Wang G. Diversity of mast cell subpopulations in the tumor microenvironment of colorectal cancer and their prognostic implications. Cancer Immunol Immunother, 2025, 74(8):255. https://doi.org/10.1007/s00262-025-04119-8 PMID: 40586903 PMCID: PMC12209079
[11] Huang S, Wu H, Luo F, Zhang B, Li T, Yang Z, Ren B, Yin W, Wu D, Tai S. Exploring the role of mast cells in the progression of liver disease. Front Physiol, 2022, 13:964887. https://doi.org/10.3389/fphys.2022.964887 PMID: 36176778 PMCID: PMC9513450
[12] Weidner N, Folkman J, Pozza F, Bevilacqua P, Allred EN, Moore DH, Meli S, Gasparini G. Tumor angiogenesis: a new significant and independent prognostic indicator in early-stage breast carcinoma. J Natl Cancer Inst, 1992, 84(24):1875–1887. https://doi.org/10.1093/jnci/84.24.1875 PMID: 1281237
[13] Frentzas S, Simoneau E, Bridgeman VL, Vermeulen PB, Foo S, Kostaras E, Nathan M, Wotherspoon A, Gao ZH, Shi Y, Van den Eynden G, Daley F, Peckitt C, Tan X, Salman A, Lazaris A, Gazinska P, Berg TJ, Eltahir Z, Ritsma L, Van Rheenen J, Khashper A, Brown G, Nystrom H, Sund M, Van Laere S, Loyer E, Dirix L, Cunningham D, Metrakos P, Reynolds AR. Vessel co-option mediates resistance to anti-angiogenic therapy in liver metastases. Nat Med, 2016, 22(11):1294–1302. https://doi.org/10.1038/nm.4197 PMID: 27748747 PMCID: PMC5104270
[14] Van den Eynden GG, Bird NC, Majeed AW, Van Laere S, Dirix LY, Vermeulen PB. The histological growth pattern of colorectal cancer liver metastases has prognostic value. Clin Exp Metastasis, 2012, 29(6):541–549. https://doi.org/10.1007/s10585-012-9469-1 PMID: 22476470
[15] Ammendola M, Marech I, Sammarco G, Zuccalà V, Luposella M, Zizzo N, Patruno R, Crovace A, Ruggieri E, Zito AF, Gadaleta CD, Sacco R, Ranieri G. Infiltrating mast cells correlate with angiogenesis in bone metastases from gastric cancer patients. Int J Mol Sci, 2015, 16(2):3237–3250. https://doi.org/10.3390/ijms16023237 PMID: 25648323 PMCID: PMC4346892
[16] Dakhel S, Padilla L, Adan J, Masa M, Martinez JM, Roque L, Coll T, Hervas R, Calvis C, Messeguer R, Mitjans F, Hernández JL. S100P antibody-mediated therapy as a new promising strategy for the treatment of pancreatic cancer. Oncogenesis, 2014, 3(3):e92. https://doi.org/10.1038/oncsis.2014.7 PMID: 24637492 PMCID: PMC4038391
[17] Soucek L, Lawlor ER, Soto D, Shchors K, Swigart LB, Evan GI. Mast cells are required for angiogenesis and macroscopic expansion of Myc-induced pancreatic islet tumors. Nat Med, 2007, 13(10):1211–1218. https://doi.org/10.1038/nm1649 PMID: 17906636
[18] Cimpean AM, Raica M. The hidden side of Disodium Cromolyn: from mast cell stabilizer to an angiogenic factor and antitumor agent. Arch Immunol Ther Exp (Warsz), 2016, 64(6):515–522. https://doi.org/10.1007/s00005-016-0408-8 PMID: 27289241

Corresponding author
Amalia-Raluca Ceauşu, Habil. Associate Professor, MD, PhD, Department of Microscopic Morphology/Histology, Angiogenesis Research Center, Victor Babeş University of Medicine and Pharmacy, 2 Eftimie Murgu Square, 300041 Timişoara, Romania; Phone +40256–204 250, e-mail: ra.ceausu@umft.ro

Received: June 15, 2026

Accepted: September 4, 2026